ANL-HEP-CP--91-95

DE92 004153

Northwestern University:
N.U.H.E.P. Report No. 191
ANL-HEP-CP-91-95
October, 1991

Review of Total Cross Sections and Forward Scattering Parameters at Ultra-High Energies

Martin M. Block *

Department of Physics and Astronomy,
Northwestern University, Evanston, IL 60208-3112

Alan R. White †

High Energy Physics Division,
Argonne National Laboratory, Argonne IL 60439

Paper presented by Martin M. Block
at the
XXI International Symposium on Multiparticle Dynamics,
Wuhan, China, Sept. 23–27, 1991

Abstract

We review the field of elastic scattering of pp and $\bar{p}p$ at ultra-high energies. The recent total cross section, σ_{tot}, and ρ-value results from the Fermilab Tevatron Collider experiments presented at the 4th 'Blois' Workshop on Elastic and Diffractive Scattering (Elba, Italy, in May, 1991), allow us a comprehensive overview of the field.

*Work partially supported by Department of Energy contract DA-AC02-76-Er02289 Task B.
†Work supported by Department of Energy Contract W-31-109-ENG-38.

I. Introduction

One of us (M. M. B.) would like to thank the Organizers, and in particular, Professor Liu Lianshou, for the opportunity to present this communication. The UA4 measurement,[1] some four years ago, of the ρ-value (the ratio of the real to the imaginary portion of the forward nuclear scattering amplitude) for $\bar{p}p$ scattering at 540 GeV produced an unexpectedly large result. The possible anomalous nature of the result was partly recognized at the time, but since there were no results from the Fermilab Tevatron, it seemed most likely that it simply anticipated a fast-increasing cross section from 'minijet' and other 'semi-hard' processes at higher energies. However, the new Tevatron results are now in hand and summarized in Table II. The cross section at 1800 GeV is, if anything, smaller than expected from low-energy extrapolations and, in general, the results conform to an overall simplicity and consistency with lower energy data, making the UA4 result distinctively anomalous. The experiment will be repeated in November as UA4/2, and, not surprisingly, the outcome of the UA4/2 experiment is very eagerly anticipated.

The field of ultra-high energy elastic scattering of pp and $\bar{p}p$ collisions is reviewed, to study the forward scattering parameters, among which are $\sigma_{\rm tot}$, the total cross section, B, the nuclear slope parameter, and ρ. We will attempt to give a critical overview of the field, including future possibilities at the LHC and SSC Colliders.

II. Review of Experimental Method

All modern elastic scattering experiments are done using colliders, with either pp or $\bar{p}p$ collisions. The detectors are place in 'Roman Pots', which are reentrant cavities (using bellows) into the collider beam pipes, into which are introduced detectors (typically, very small drift chambers) to gather coincident collisions. This is done in order to get to the *very small* angles needed to detect the low $|t|$ collisions (t is the squared 4-momentum transfer, and for a collider, is given by $t = -(p\theta)^2$) that are of critical importance in this work. Following the review of Block and Cahn,[2] we introduce the invariant scattering amplitudes

$$F_c = (\mp)\frac{2\alpha G^2(t)\sqrt{\pi}}{|t|} \quad \text{and} \quad F_n = \frac{(\rho + i)\,\sigma_{\rm tot}\, e^{Bt/2}}{4\sqrt{\pi}}, \tag{1}$$

for Coulomb and nuclear scattering, respectively, and where the upper sign is for pp and the lower sign is for $\bar{p}p$. However, the simultaneous presence of the Coulomb *and* the nuclear interactions require us, *not* to add amplitudes directly, but to introduce a phase $\alpha\phi(t)$,[3] such that

$$\begin{aligned} \frac{d\sigma}{dt} &= \frac{d\sigma_c}{dt} + \frac{d\sigma_{cn}}{dt} + \frac{d\sigma_n}{dt} = \left|F_c e^{i\alpha\phi(t)} + F_n\right|^2 \\ &= \pi\left|(\mp)G^2(t)\frac{2\alpha}{|t|}e^{i\alpha\phi(t)} + (\rho + i)\frac{\sigma_{\rm tot}}{4\pi}e^{Bt/2}\right|^2. \end{aligned} \tag{2}$$

In the above, α is the fine-structure constant ($\approx 1/137$), and $G^2(t)$ is the dipole form factor taken from electron-proton scattering (for our purposes, it can be taken as unity). The phase $\alpha\phi(t)$ is almost independent of t, and is small—about 0.02. We define $|t|_{\rm int}$ and $\theta_{\rm int}$ as the t-value and scattering angle, respectively, where the Coulomb and nuclear amplitudes are equal, *i.e.*, the region of *maximal* interference. The $|t|$-values much below $|t|_{\rm int}$ give rise to the Coulomb region of scattering ($d\sigma_c/dt$), the values much above give rise to the nuclear region ($d\sigma_n/dt$), and the region near $|t|_{\rm int}$ is called the interference region($d\sigma_{cn}/dt$). An ideal experiment would achieve its absolute normalization (conversion of counting rate into cross section) from the Coulomb region, where the (known) Coulomb cross section predominates. Using the optical theorem, it would get the total cross section $\sigma_{\rm tot}$ from the extrapolation of the elastic differential cross section from the nuclear region back to $t = 0$, *i.e.*, $d\sigma_n/dt|_{t=0}$, which measures $\sigma_{\rm tot}(1+\rho^2)^{1/2}$. The data near $|t|_{\rm int}$ determine the ρ value. This is seen since the interference term of Eq (2), $d\sigma_{cn}/dt$, can be simplified in the small t-region to be

$$\frac{d\sigma_{cn}}{dt} \approx 2(\rho+\alpha\phi)F_cF_n \approx (\mp)(\rho+\alpha\phi)\left[\frac{\alpha\sigma_{\rm tot}}{|t|}\right], \tag{3}$$

and hence is a direct measure of ρ.

To get an idea of the t-scale and the minimum angle $\theta_{\rm min}$ needed experimentally at a collider, we show the values of $|t|_{\rm int}$ and $\theta_{\rm int}$ for the Coulomb interference region for $p\bar{p}$ scattering in Table I, taken from the review article of Block and Cahn.[2] We note that the value of $\theta_{\rm int}$ for the SSC is seen to be about 1 microradian, a very small value, indeed. In order to achieve it, a β^*-section of the order of several *kilometers* must be installed in the SSC.

Table I: Values of $|t|_{\rm int}$ and $\theta_{\rm int}$ for the Coulomb interference region for $p\bar{p}$ scattering.

$\sqrt{s}$ (GeV)	Accelerator	$\lvert t\rvert_{\rm int}$ $(\mathrm{GeV/c})^2$	$\theta_{\rm int}$ (mrad)
62.5	ISR	0.0016	1.3
540	S$\bar{p}$pS	0.0010	0.12
2000	Tevatron Collider	0.00073	0.027
40000	SSC	0.00037	0.00097

Another method of normalization is to measure directly the luminosity $\mathcal{L}$ of the collider. The experimenter, using this technique, measures the combination $\sigma_{\rm tot}(1+\rho^2)^{1/2}$.

Still another method is commonly used, the so-called 'Luminosity Free' technique, where one simultaneously measures $dN_n/dt|_{t=0}$, the elastic nuclear counting rate extrapolated to $t = 0$, and N_{total}, the total number of events (inelastic plus elastic).

This allows one to measure the quantity $\sigma_{tot}(1+\rho^2)$. The advantage is that it frees the experimenter from having to make an absolute direct measurement of the machine luminosity, a difficult task at the S$\bar{p}$pS and Tevatron Colliders.

The E710 group,[4] using this last technique and getting well into the interference region, has made simultaneous measurements of σ_{tot}, ρ and B, the nuclear slope parameter of Eq (2), and has presented their results from the Tevatron Collider at $\sqrt{s} = 1800$ GeV at the Elba, Italy, Conference last May. The CDF group[5] also presented results at 1800 GeV, using the method where they measured directly the machine luminosity. Since they were at larger $|t|$ values than E710, they were only able to measure in the nuclear region, and thus, presented results for σ_{tot} and B, only. The Tevatron results at $\sqrt{s} = 1800$ GeV are summarized in Table II.

Table II: Experimental results at the Tevatron Collider at $\sqrt{s} = 1800$ GeV.

	σ (mb)	B $(\mathrm{GeV/c})^{-2}$	ρ	$\sigma_{elastic}/\sigma_{tot}$
E710	72.8 ± 3.1	16.99 ± 0.47	0.140 ± 0.069	0.223 ± 0.012
CDF	72.0 ± 3.6	16.50 ± 0.76		0.229 ± 0.020

III. Simplicity and the Regge Pole Picture

In Figs. 1–3, we show the latest results from E710[4] and CDF[5] on measurements of σ_{tot}, B and ρ for $\bar{p}$p scattering at the Tevatron collider, along with the available lower energy data. It does not take a 'trained eye' to see that a 'linear' (in $\log s$) fit to the high-energy behavior of both σ and B would not be bad—over an $\sqrt{s}$ range of several orders of magnitude for the slope and almost two orders of magnitude for the cross section! The indicated theoretical curves (for a QCD eikonal model) will be discussed later in Section V.

The simplicity of the plot for B for pp is particularly striking. Since a logarithmically increasing slope parameter is well-known to be directly associated with a single Pomeron Regge pole having a linear trajectory, it is very hard to study this plot and not conclude that a simple Regge pole must be an excellent first approximation to the Pomeron. The slope of the Pomeron Regge trajectory appears explicitly in the energy dependence of the slope parameter, *i.e.*,

$$B = B_0 + 2\alpha' \log s,, \tag{4}$$

and the value $\alpha' = 0.2$ gives a satisfactory fit to the pp data.

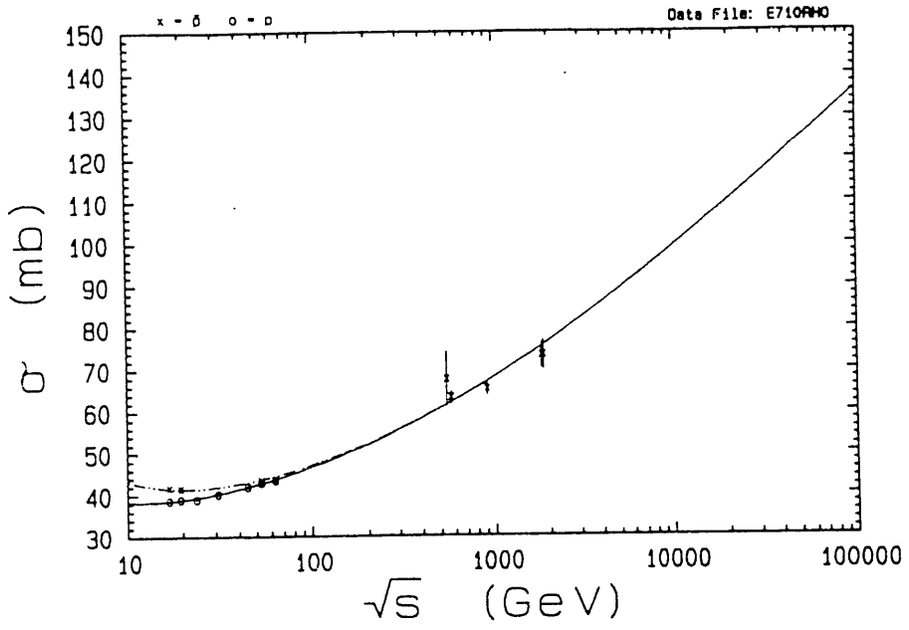

Figure 1: $\sigma_{\rm tot}$, the calculated and measured total cross sections, for $\bar{\rm p}$p (dashed curve and crosses) and pp (full curve and circles), *vs.* $\sqrt{s}$, the energy.

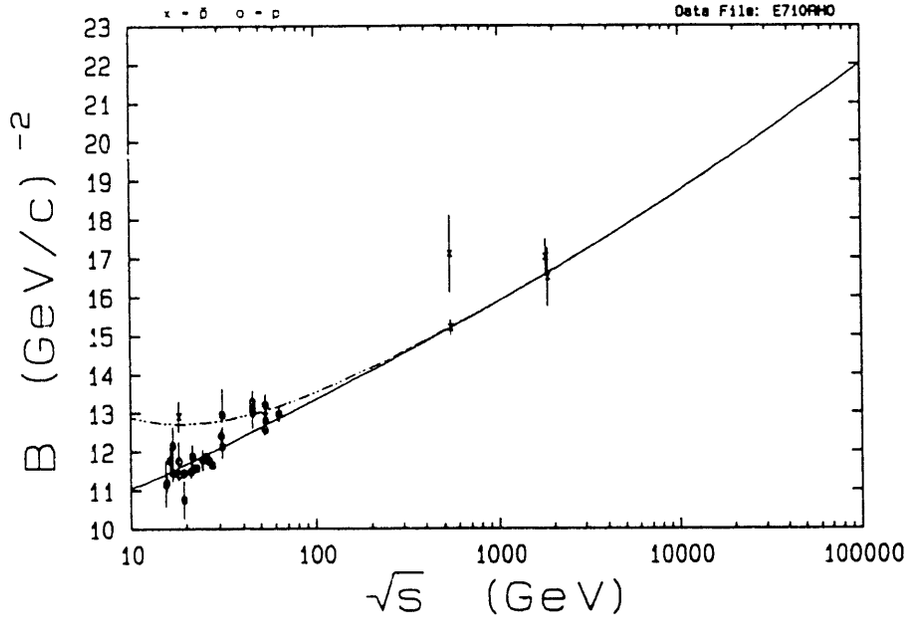

Figure 2: B, the calculated and measured nuclear slope parameters, for $\bar{\rm p}$p (dashed curve and crosses) and pp (full curve and circles) *vs.* $\sqrt{s}$, the energy.

Since a Regge pole gives a power behavior for the total cross section, the 'logarithmic' behavior of Fig. 1 has to be numerically reproduced by a small power, if this is a valid picture. The very simple curve

$$\sigma_{\rm tot} = 22\ s^{0.08}\ {\rm mb}, \tag{5}$$

turns out to be a rather good approximation to the energy dependence of the total cross section. Thus, a simple Regge pole amplitude with Regge trajectory

$$\alpha(t) = 1.08 + 0.2\,t \tag{6}$$

provides a remarkable first approximation to near-forward elastic scattering from ISR energies to the Tevatron Collider.[6] It is equally remarkable that this effective trajectory had already been extracted from the earliest ISR pp scattering data.[11]

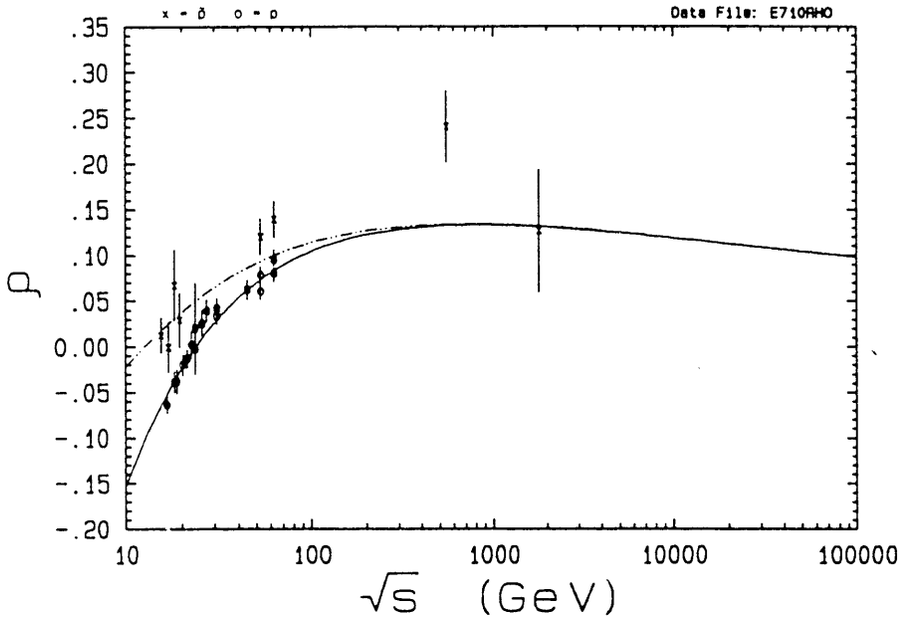

Figure 3: ρ, the calculated and measured ratios ${\rm Re}f(0)/{\rm Im}f(0)$, for $\bar{\rm p}$p (dashed curve and crosses) and pp (full curve and circles), *vs.* $\sqrt{s}$, the energy.

If Eq (5) provides the total cross section, the corresponding real amplitude Re $A_{\rm pp}$ (which is here taken to be equal to Re $A_{\bar{\rm p}{\rm p}}$) is easily obtained from the asymptotic dispersion relation

$$\frac{{\rm Re}\ A_{\rm pp}}{s} = \frac{\pi}{2}\,\frac{d\sigma_{\rm tot}}{d(\log s)} + O[\frac{d^2\sigma_{\rm tot}}{d(\log s)^2}] = \frac{\pi}{2} \times 0.08 \times \sigma_{\rm tot}\ + \ \ldots, \tag{7}$$

where we have used the normalization σ = Im A/s. From Eq (7) and the above normalization, we infer that ρ, the ratio of the real to the imaginary portion of the forward nuclear scattering amplitude, is given by

$$\rho = \frac{\pi}{2} \times 0.08 \approx 0.12. \tag{8}$$

Thus, a single Regge pole amplitude should have an essentially constant value of ρ. Data for ρ from $\bar{p}$-p and p-p scattering are plotted in Fig. 3, including the recent preliminary result from E710.[4] The anomalous nature of the UA4 result is now apparent. The high-energy results are roughly consistent with the simple Regge pole value of Eq (8), apart from the UA4 value of 0.24, which is *twice* what we expect from Eq (8)! This conclusion is not particular to the Regge pole amplitude employed, as we shall discuss further in succeeding Sections. It is an inevitable consequence of assuming that the energy dependence of amplitudes is smooth, and that Eq (7) is valid. The Regge pole amplitude is just the simplest approximation to all near-forward elastic data (apart from the UA4 value for ρ) which satisfies the necessary analyticity constraints. The asymptotic Froissart bound is, of course, not satisfied by Eq (5), and we shall address this point in Section V.

We consider now the t-dependence of the elastic differential cross section away from the very forward direction. At modest t, we encounter the presence of curvature, or more dramatically, what used to be called the 'break in slope' around $|t| = 0.1$ (GeV/c)^2. The nuclear slope parameter B and the nuclear curvature C are defined, in terms of the elastic scattering cross section $d\sigma/dt$, by $B = \frac{d}{ds}[\log(d\sigma/dt)]_{t=0}$ and $C = \frac{1}{2}\frac{d^2}{ds^2}[\log(d\sigma/dt)]_{t=0}$, respectively. The data for $d\sigma/dt$ show a break (by about 2 units in B, where B is in (GeV/c)^2) at the ISR, *i.e., positive* curvature, getting smaller at the S$\bar{p}$p, in the low $|t|$ interval, $|t| < 0.65$ (GeV/c)^2. The effect seems to have almost disappeared at the Tevatron collider. E710[12] reports an analysis in which they measure the curvature C to be consistent with *zero*. Their experimental data are shown in Fig. 4, along with the QCD-prediction of Section V.

In the Regge pole picture we have so far described, the t-dependence is that of a constant slope with *no* curvature, 'shrinking' logarithmically with increasing energy. To introduce curvature into $\frac{d\sigma}{dt}$, one modifies either the Regge residue or the Regge Pole trajectory. The former gives an energy *independent* curvature, whereas the latter gives curvature which *increases logarithmically* with energy. In either case, the curvature *can not disappear*, as indicated by the E710 results, or *reduce in magnitude*, as already suggested by the comparison of the S$\bar{p}$pS results with the ISR data. This poses a serious contradiction for this formalism, which is not readily resolvable.

We conclude therefore that while the data almost conform to a very simple picture of a Regge pole Pomeron:

(A) the UA4 forward real part

(B) the disappearance of curvature at $|t| \approx 0.1$ (GeV/c)^2 at $\sqrt{s} = 1800$ GeV

(C) the energy dependence of the $\bar{p}$p large $|t|$ data

all present serious problems for this simple picture. Of these effects, perhaps the most critical is (B), the lack of explanation of the vanishing of the small $|t|$ curvature with increasing energy. In contrast, these effects are rather naturally explained in the eikonal picture, summarized in Section V.

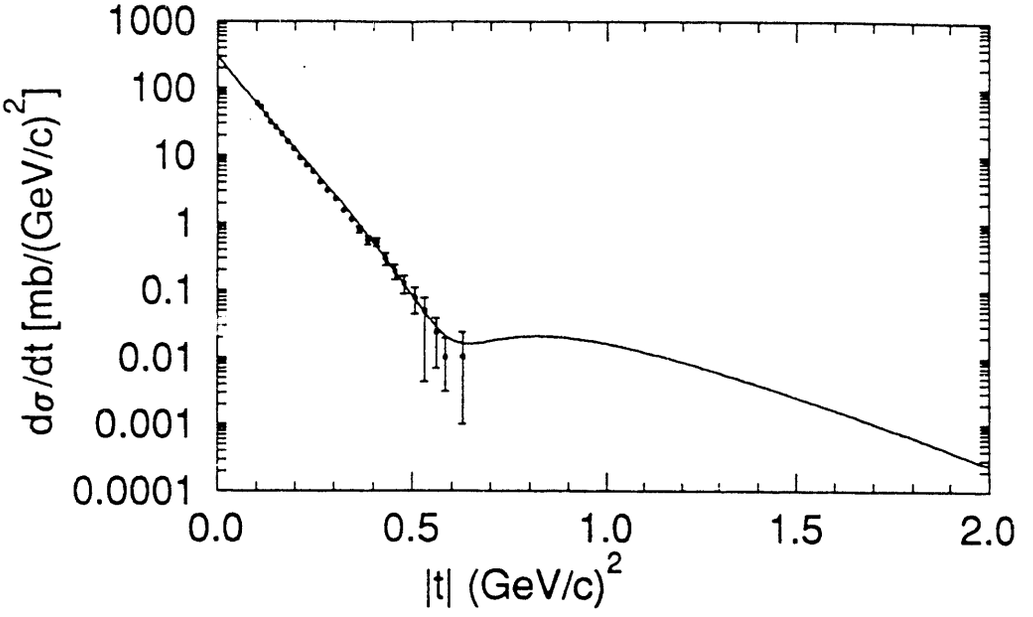

Figure 4: The differential cross section $d\sigma/dt$ *vs.* $|t|$, for $\bar{p}p$ at $\sqrt{s} = 1800$ GeV. The solid curve is the prediction of Ref. 8, based on a QCD model of soft interactions, and the experimental data are from the E710 Collaboration[12]. This figure was taken from Ref. 9.

IV. True Asymptopia—Could we be There?

If the Regge pole Pomeron of the last Section is a good first approximation, then true asymptopia is way *beyond any* ever *attainable* energy scale. We now switch from this extreme to the other extreme, *i.e.*, discussing whether we may actually already be in asymptopia. Later, we shall discuss possible intermediate situations. We consider the outcome of applying a standard asymptotic analytic amplitude analysis procedure to the data on the total cross section $\sigma_{\rm tot}$ and ρ. While there is ample physical argument that we are *not* in asymptopia, the virtue of the analytic amplitude formalism is that it allows a phenomenological analysis to be carried out in a well-defined framework in which specific hypotheses can be made and tested.

The analysis parameterizes the data in terms of even and odd analytic amplitudes, consistent with all asymptotic theorems. In particular, the Froissart bound is imposed, in terms of the power dependence on $\log s$ that is considered. This allows for even amplitudes varying as fast as $\log^2(s/s_0)$, where s_0 is a scale for s, and odd amplitudes (the 'Odderon' family) that do *not* vanish as $s \to \infty$. Details of the analysis can be found in Ref. 7. Here we simply note some of the key features.

The large s limit of the even and odd amplitudes used is as follows. We introduce the $\bar{p}p$ and pp forward scattering amplitudes by

$$f_{\bar{p}p} = f_+ + f_- \quad \text{and} \quad f_{pp} = f_+ - f_-, \tag{9}$$

where f_+ and f_- are even and odd (under crossing) analytic amplitudes at $t = 0$.

The total cross sections σ_{tot} and the ρ-values are given by:

$$\sigma_{\bar{p}p} = \frac{4\pi}{p}\,\mathrm{Im}\,f_{\bar{p}p} \quad \text{and} \quad \sigma_{pp} = \frac{4\pi}{p}\,\mathrm{Im}\,f_{\bar{p}p} \tag{10}$$

$$\rho_{\bar{p}p} = \frac{\mathrm{Re}\,f_{\bar{p}p}}{\mathrm{Im}\,f_{\bar{p}p}} \quad \text{and} \quad \rho_{pp} = \frac{\mathrm{Re}\,f_{pp}}{\mathrm{Im}\,f_{pp}}. \tag{11}$$

The 'conventional' even and odd amplitudes f_+ and f_- are parameterized as (*c.f.* Eq (5.2a-b) of Ref. 2):

$$\frac{4\pi}{p}f_+ = i\left(A + \beta\left[\log\left(\frac{s}{s_0}\right) - i\frac{\pi}{2}\right]^2 + c\,s^{\mu-1}e^{i\pi(1-\mu)/2}\right) \tag{12}$$

$$\frac{4\pi}{p}f_- = -Ds^{\alpha-1}e^{i\pi(1-\alpha)/2}. \tag{13}$$

We will find that α in Eq (13) is about 0.5, and hence, this odd amplitude vanishes as $s \to \infty$. Since asymptotic theorems[13,14] show that the *difference* of cross sections can not grow faster than $\log^{\gamma/2}s$ if the cross section grows as $\log^{\gamma}s$, the prototypical odd amplitudes which do *not* vanish as $s \to \infty$ for this case are (*c.f.* Eq (5.8a–c) of Ref. 2): [15,16,17]

$$\frac{4\pi}{p}f_-^{(0)} = -\epsilon^{(0)} \tag{14}$$

$$\frac{4\pi}{p}f_-^{(1)} = -\left[\log\left(\frac{s}{s_0}\right) - i\frac{\pi}{2}\right]\epsilon^{(1)} \tag{15}$$

$$\frac{4\pi}{p}f_-^{(2)} = -\left[\log\left(\frac{s}{s_0}\right) - i\frac{\pi}{2}\right]^2\epsilon^{(2)}. \tag{16}$$

We form the complete odd amplitude by adding any *one* of the $f_-^{(i)}$ of Eq (14–16) to the conventional odd amplitude f_- of Eq (13).

We first consider the case of no Odderon. The computed curves are shown in Fig. 5 (for σ_{tot}) and Fig. 6 (for ρ). The pp cosmic-ray lower limit[24] is appended to the curve, but is *not* used in the fit. [The parameters of all the fits we discuss are given in Ref. 7].

The most obvious features of the fit are:

(A) it goes far above the measured total cross section (E710) at 1800 GeV, which is the highest energy point measured to date (the predicted value is too high to fit the experimental value by more than a 3σ deviation),

(B) it is about 1.5σ below the UA4 ρ-value at 546 GeV.

We next attempt to fit the data by adding an additional degree of freedom, *i.e.*, adding Odderon 2 of Eq (16) to f_- of Eq (13), along with the even amplitude of Eq (12). These curves are shown in Figs. 7 and 8.

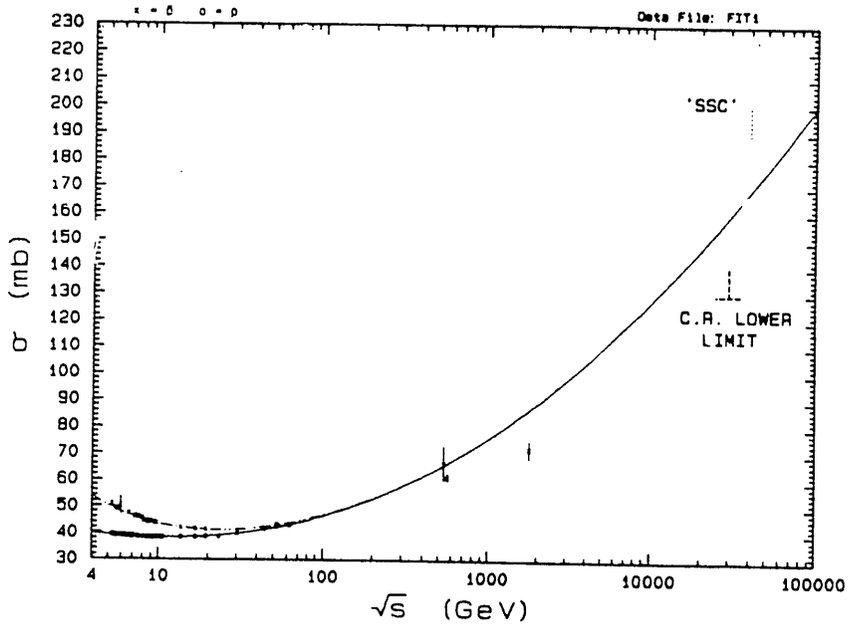

Figure 5: The total cross section σ_{tot}, in mb *vs.* the energy, $\sqrt{s}$, in GeV. The fit was made with a $\log^2 s$ energy variation, and no Odderon. Crosses indicate $\bar{p}p$ and the circles pp data. The dot-dashed curves are for $\bar{p}p$, and the solid curves for pp.

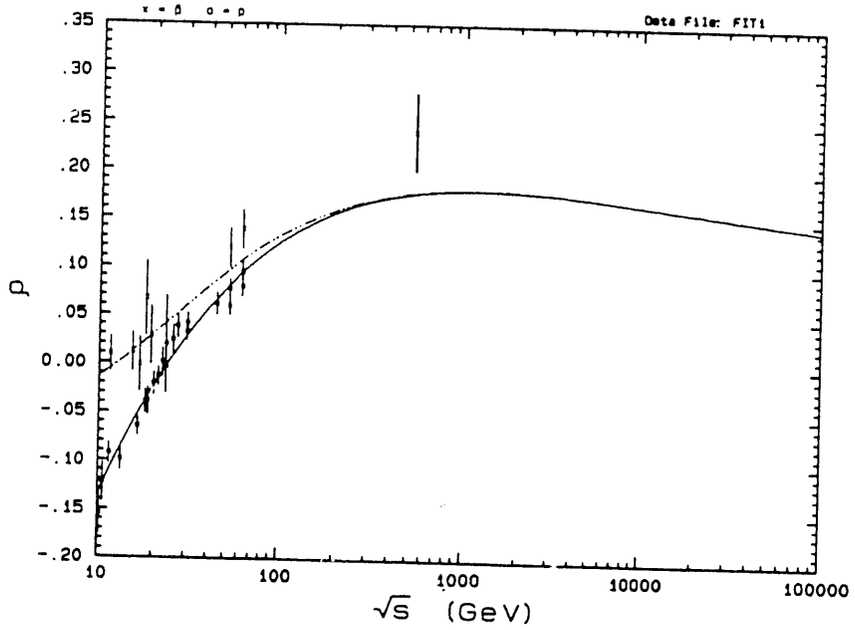

Figure 6: The ρ-value for $\bar{p}p$ and pp scattering *vs.* the energy, $\sqrt{s}$, in GeV. The fit was made with a $\log^2 s$ energy variation, and no Odderon.

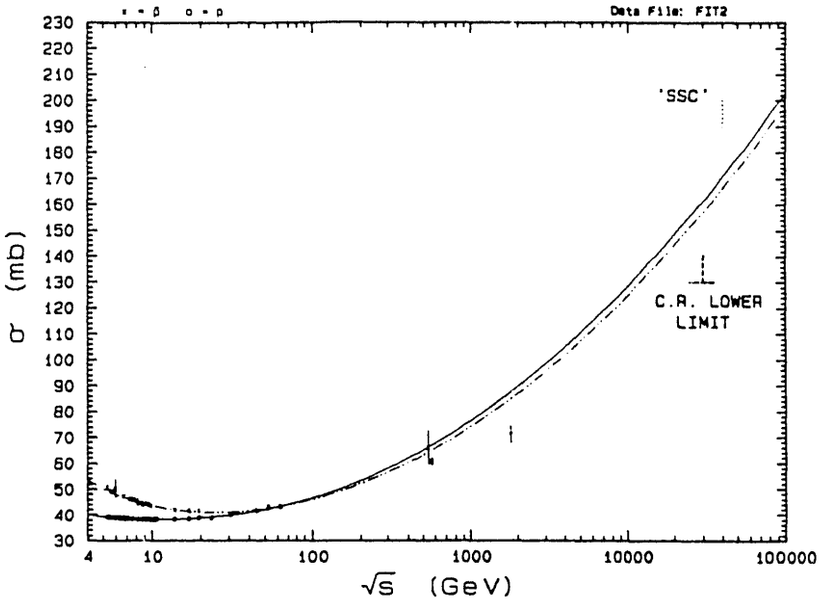

Figure 7: The total cross section σ_{tot}, in mb, for $\bar{p}p$ and pp scattering *vs.* the energy, $\sqrt{s}$, in GeV. The fit was made with a $\log^2 s$ energy variation, and used Odderon 2.

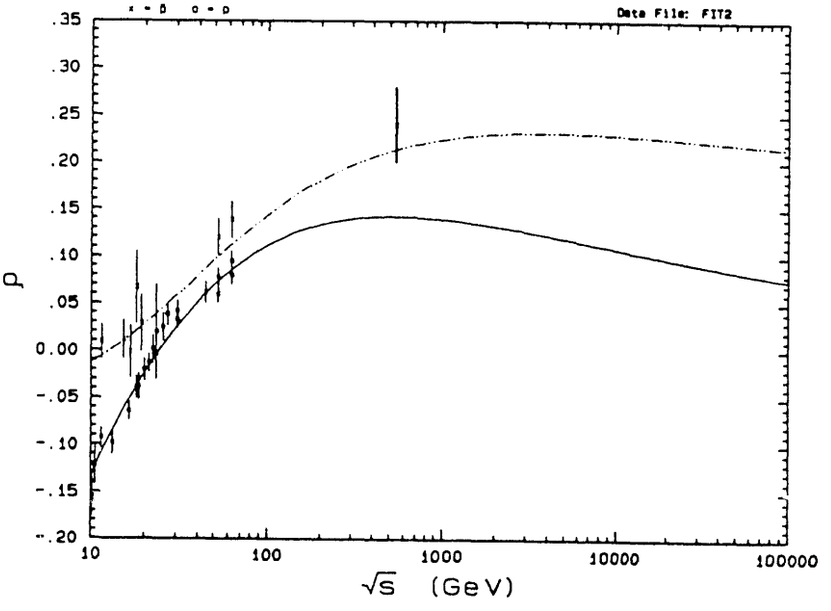

Figure 8: The ρ-value for $\bar{p}p$ and pp scattering *vs.* the energy, $\sqrt{s}$, in GeV. The fit was made with a $\log^2 s$ energy variation, and used Odderon 2.

The high energy cross section predicted at 1800 GeV is again much too high (3.4σ), although the ρ-value predicted at 540 GeV is now satisfactory. The Odderon amplitude $\epsilon^{(2)} = -4.5 \pm 1.5 \times 10^{-2}$ mb (from Ref. 7) is very tiny compared to the other amplitudes, and therefore, can't do very much to the fit. The fit with Odderon 1 of (15) is also reported in Ref. 7. Since an Odderon of this type does even less to the fit, we do not show the results here.

We now consider the scale factor s_0 in Eqs (15) and (16) to be *different* from the scale factor in the conventional even amplitude of Eq. (12) and replace it by a new scale s_1. We repeated the fit described above for Odderon 2 (Fit # 2), adding the *additional* parameter s_1. Qualitatively, the fit did not change, and we see no necessity for the new scale. Our general conclusion, at this point, is that an even amplitude varying as $\log^2(s/s_0)$ does *not* fit the high-energy cross section data. The addition of an Odderon term does nothing to ameliorate this difficulty.

We next consider an asymptotic variation that goes as $\log s$. For this purpose, we substitute for the even amplitude in Eq (12) a new amplitude which varies as $\log s$ (*c.f.* Eq (5.7) of Ref. 2):

$$\frac{4\pi}{p} f_+ \;=\; i\left(A + \beta\left[\log\left(\frac{s}{s_0}\right) - i\frac{\pi}{2}\right] + c\, s^{\mu-1} e^{i\pi(1-\mu)/2}\right). \tag{17}$$

We use the conventional odd amplitude of Eq (13), along with no Odderon or Odderon 1. We emphasize the point made above that since the energy variation of the cross section is now only $\log s$, Odderon 2 is *not* allowed by the asymptotic theorems.

The fit for σ_{tot} with no Odderon is shown in Fig. 9. It is quite satisfactory, fitting reasonably well to all cross section data over the entire range of energy. With the exception of the UA4 point at 546 GeV, it also fits the ρ-values.[7] However, it predicts a ρ-value at 546 GeV that is 0.13, compared to the measured value of 0.24 ± 0.04, about a 2.7σ effect. Note that the preliminary E710 value of ρ was not included in any of the fits. However, it is clearly consistent with the prediction. We note, but do not show, that (also not surprisingly) the fit with Odderon 1 is almost indistinguishable from the fit without it.

We conclude:

(A) the cross section can be fit with a $\log(s/s_0)$ variation. Because of the dominance of low energy points, we interpret the failure of the $\log^2(s/s_0)$ fit as implying that a fit of this kind to data at ISR energies and below will *not* fit the *new high-energy* cross section data. This surely means that there is no basis for the statement (often made in the past) that the cross section is rising like the $\log^2 s$ maximal behavior allowed by the Froissart bound. It is important to emphasize, however, that this analysis *does not exclude* either models which contain $\log^2 s$ behavior with a small coefficient or models that develop a $\log^2 s$ behavior at a higher energy scale.

(B) the UA4 ρ-value can *not* be fit, either *with* or *without* an Odderon. In this context, the Odderon hypothesis (interpreted *strictly* as the presence of an *asymptotic* odd-signature amplitude) is *irrelevant* to the problem of fitting the UA4 ρ-value.

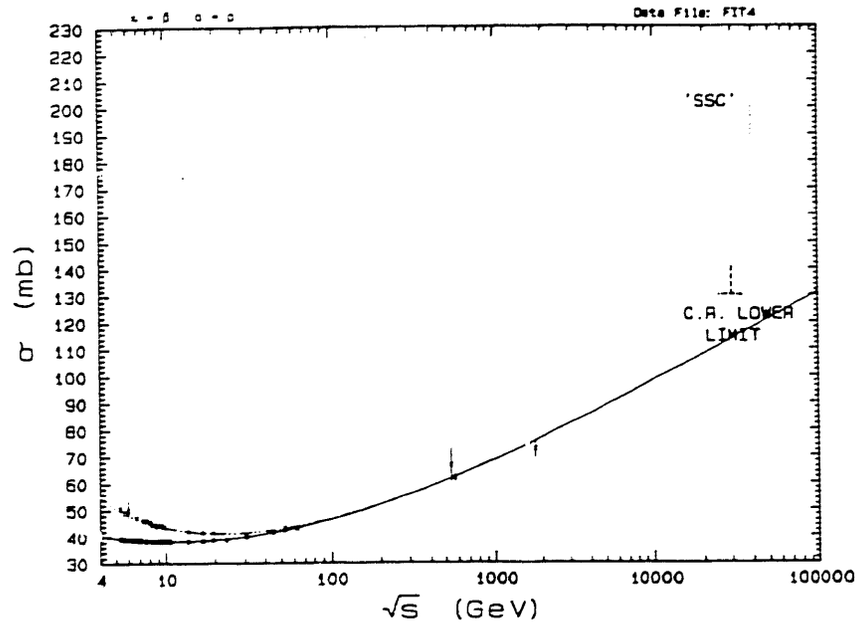

Figure 9: The total cross section σ_{tot}, in mb, for $\bar{p}p$ and pp scattering *vs.* the energy, $\sqrt{s}$, in GeV. The fit was made with a $\log s$ energy variation, and no Odderon.

V. S-Channel Unitarity and QCD

A fully unitary theory must, of course, satisfy full multiparticle unitarity in both the s-channel and the t-channel. The eikonal formalism provides essentially the only practical method for implementing the idea that s-channel unitarization effects play a major role.

The eikonal formalism starts by writing the exponential representation of the amplitude $A(s,t)$, as an integral over impact parameter space b,

$$A(s,t) = is \int d^2b \; J_0(b\sqrt{-t}) \left[1 - e^{-\chi(b,s)}\right], \tag{18}$$

where $\chi(b,s)$ will be referred to as the eikonal in the following.

In order to understand the general properties that *most* eikonal models share, we now introduce a simple, factorizable eikonal, which has a power-law s dependence,

$$\chi(b,s) = W(b)s^a, \tag{19}$$

with $a > 0$, and where $W(b)$, the impact parameter space description, is given by

$$W(b) = K_3(\mu b)(\mu b)^3, \tag{20}$$

with K_3 being the modified Bessel function. The mass μ sets the scale of the variation in b-space, and is the mass occurring in the dipole form factor description $G(q^2) = \frac{1}{(1+q^2/\mu^2)^2}$ given by the Durand-Lipes modification[18] of the Chou-Yang model.[19] Each

term in the eikonal series given by Eq (19) strongly violates the Froissart bound.[20] However, ever since the work of Cheng and Wu,[21] it has been understood that the Froissart bound is restored as a consequence of the strong cancellations between the terms of the series. As a result, the full amplitude generated by the eikonal of Eq (19) does indeed satisfy the Froissart bound (see Eqs (27–31) below for a heuristic derivation).

It has long been known from asymptotic theorems[23] that when the maximal energy dependence allowed by the Froissart bound is achieved, the differential cross section satisfies

$$\frac{d\sigma}{dt} \longrightarrow \left[\log^2 s \; F(t\log^2 s)\right]^2 \approx \left[\log^2 s \; \{F(0) + F'(0)\, t \log^2 s + \cdots\}\right]^2 . \tag{21}$$

We recall that the nuclear slope parameter B is given, in terms of the elastic scattering cross section $d\sigma/dt$, by $B = \frac{d}{ds}[\log(d\sigma/dt)]_{t=0}$. Thus, Eq (21) yields

$$B \;=\; 2\left[\frac{F'(0)}{F(0)}\right]\log^2 s, \tag{22}$$

and hence, 'shrinkage' of the diffraction pattern with increasing energy. Although this effect is *not* present in any term of the series of Eq (18), it emerges from the exponentiation process.

It is easy to show that at small s, the eikonal in Eq (19) gives a *positive* curvature C, because of the shape of the dipole form factor being important when the eikonal is small. However, as the energy becomes very large, it is easy to show[2] that the amplitude becomes that of a sharp disk, and that, asymptotically, $B = R^2/4$ and $C = -R^4/192$, where $R = R_0 \log s$. Thus, the curvature must go through zero as s increases, and eventually grow large and negative. The energy at which this zero occurs has been considered to be the onset of the transition to 'asymptopia' by Block and Cahn.[2] We note that the evolution of the curvature from positive to negative is thus a general property of most eikonal models. A typical evolution of both the slope and curvature parameters is illustrated using the QCD-inspired model of Block, Halzen and Margolis[8,9,22] (referred to hereafter as the BHM model) in Fig. 10. As can be seen, the curvature does indeed change sign at an energy close to that of the Tevatron Collider. This is born out by the experimental data, since E710 measures a curvature[12] compatible with zero at the Tevatron Collider (see Fig. 4).

In the BHM model,[8,9,22] the eikonal function is written as

$$2\chi(b,s) = W(b)\sigma(s) = P(b,s), \tag{23}$$

where $P(b,s)$, the probability of collision, is assumed to be

$$P_{ij}(b,s) = W_{ij}(b)\sigma_{ij}^{QCD}(s). \tag{24}$$

In particular, they parameterize the low energy data in terms of quark-quark (qq) and quark-gluon (qg) interactions in the eikonal as $P_{qq} = W(\mu_{qq}b)\;[a + bm_0/\sqrt{s}]$ and $P_{qg} = W(\sqrt{\mu_{qq}\mu_{gg}}b)\;[a' + b'\log s/m_0^2]$. For the glue-glue ($gg$) contribution, they take

$$\sigma_{gg}^{QCD}(s) = \int d\left(\frac{\hat{s}}{s}\right)\; F_{gg}\left(x_1x_2 = \frac{\hat{s}}{s}\right)\sigma_{gg}(\hat{s}). \tag{25}$$

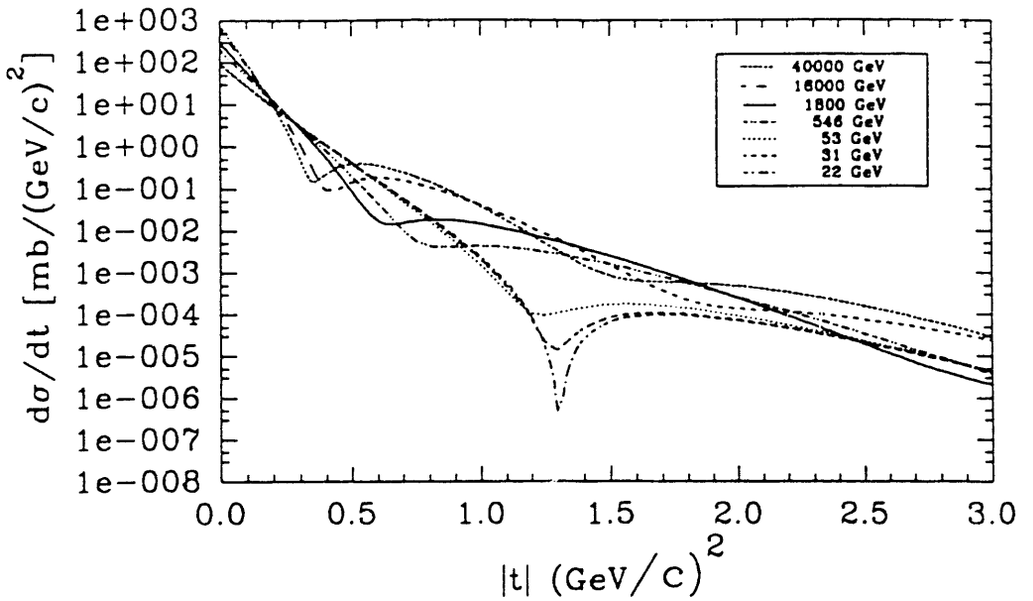

Figure 10: Evolution with energy of the differential cross section in the large $|t|$ range—according to the eikonal model of Block, Halzen and Margolis.[8,9,22]

Introducing the new variable τ via $\hat{s} = \tau s = x_1 x_2 s$, *i.e.*, the subprocess c.m. energy squared, into Eq (25), they write

$$F_{gg} = \int dx_1 dx_2 g(x_1) g(x_2) \delta(x_2 x_2 - \tau), \tag{26}$$

where $g(x) \sim \frac{(1-x)^5}{x^J}$ is the gluon structure function. The crucial quantity is J which controls the evolution of the gluon structure at small x. In Regge language, J is the intercept of the Pomeron. The factor in Eq. (25) determining the energy dependence is $\int_{m_0^2/s}^1 d\tau F_{gg}(\tau)$. One obtains, for large enough s,

$$\int_{m_0^2/s}^1 d\tau F_{gg}(\tau) \sim \int_{m_0^2/s}^1 d\tau \frac{-\log \tau}{\tau^J} \sim \left(\frac{s}{m_0^2}\right)^{J-1}. \tag{27}$$

Note that F_{gg} in Eq (27) counts the number of gluons in the colliding hadrons. The number increases rapidly at $x \simeq m_0/\sqrt{s}$ and this is the origin of the rising cross section. More quantitatively, the probability is $P_{gg}(b,s) \sim W_{gg}(b) s^{J-1}$, which is the same as Eq (19) (where $a = J-1$), given in the general eikonal arguments above. For an interaction probability $P_{gg} \ll 1$, the energy dependence of the amplitude is given by a Pomeron pole-type power law s^{J-1}, *i.e.*, the Regge Pole amplitude associated with the trajectory of Eq (6) of Landshoff and Donnachie.[6] When the number of gluons becomes large, P_{gg} exceeds unity for a *critical* impact parameter, b_c, given by

$$c W_{gg}(\mu_{gg} b_c) s^{J-1} \sim 1, \tag{28}$$

where c is a constant.

For large values of μb, Eqs. (20) and (28) yield the following value of b_c,

$$c'(\mu_{gg} b_c)^{3/2} e^{-\mu_{gg} b_c} s^{J-1} \sim 1, \tag{29}$$

with c' another constant, and therefore,

$$b_c = \frac{J-1}{\mu_{gg}} \log \frac{s}{s_0} + O\left(\log \log \frac{s}{s_0}\right). \tag{30}$$

The large number of gluons turns the nucleon into a sharp disk of radius b_c. We note the cardinal role of J in determining the energy behavior, since J controls the increase of the number of gluons. In summary, the energy dependence of the cross section transforms from s^{J-1} at low energy, to the disk cross section

$$\sigma_{tot} = 2\pi \left(\frac{J-1}{\mu_{gg}}\right)^2 \log^2 \frac{s}{s_0}, \tag{31}$$

as $s \to \infty$. We thus reproduce the Froissart bound from QCD arguments as long as $J > 1$. The usual Froissart bound coefficient of the $\log^2 \frac{s}{s_0}$ term, $1/m_\pi^2 = 20$ mb, is here replaced by $((J-1)/\mu_{gg})^2 \sim 0.002$ mb, which now agrees with experiment! We observe that μ_{gg} controls the size of the area occupied by the gluons inside the nucleon.

The correct analyticity properties of the amplitudes are assured by substituting $s \to s e^{-i\pi/2}$ for s in the even amplitudes described above. Also, an *ad hoc* crossing odd amplitude parameterizing the difference between the pp and $p\bar{p}$ scattering amplitudes is introduced as $P_{odd} = W(\mu_{odd} b) a'' \frac{m_0}{\sqrt{s}} e^{-i\pi/4}$.

The experimental observables are calculated from $P(b,s)$ and $\sigma_{tot} = 4\pi \text{ Im } f_N$ and $\frac{d\sigma}{dt} = \pi |f_N|^2$, with

$$f_N = i \int b\, db\, J_0(b\sqrt{-t}\,) \left[1 - e^{-P_{total}(b,s)/2}\right]. \tag{32}$$

The results of fitting to the data, including the new Tevatron results, are shown in Figs 1-3, for $\sigma_{\rm tot}$, ρ and B, respectively. The predictions for the elastic scattering cross section $d\sigma/dt$ are shown in Figs. 4 and 10.

We note that a simple energy-dependent modification of the Chou-Yang model has long been known[2] to provide (qualitatively) all the energy dependent features of the diffraction pattern that we have discussed. This particular model suffers from the criticism that it has incorrect analyticity properties and makes no reference to the parton model contributions thought to be associated with QCD. In a certain sense, the BHM model can be regarded as a modern version of the Chou-Yang model which corrects these defects, and which illustrates well the straightforward capability of the eikonal model to provide a good understanding of all elastic scattering data—again with the exception of the UA4 ρ-value and the large $|t|$ $\bar{\rm p}$-p scattering at the ISR.

We finally return to the vanishing of the curvature at $\sqrt{s} = 1800$ GeV, found both experimentally[12] and in BHM.[8,9,22] These authors find that the real portion of

the eikonal in Eq (18) is dominated at *low energy* by the quark-quark contribution, and at *high energy* by the gluon-gluon interaction, with the contribution from quark-gluon scattering being rather small. It is most interesting to note that at $\sqrt{s} = 1800$ GeV, the contributions to the real portion of the 'QCD'-eikonal from quark-quark scattering and gluon-gluon scattering are *approximately equal* at $b = 0$. If this is not a numerical artifact, it provides a natural explanation for the concept of 'onset of asymptopia' occurring at this energy.

VI. Future Prospects

The UA4 value for ρ remains as the most intriguing result in the field. As we emphasize, no standard formalism is able to reproduce it—even the most general eikonal model. It could even be a unique signature of a threshold for new exotic physics, as pointed out by Kang and White.[10] This result should be available in the near future.

However, we note from our above arguments that we do *not* get into 'asymptopia' until we get to energies considerably above 2 TeV. Thus, the LHC and SSC, at 16 and 40 TeV, respectively, will play a critical role in our understanding of high energy phenomena. To this end, Block, Halzen and Margolis[22] have made 'QCD'-predictions

Table III: Collider cross section predictions, with upper and lower bounds, using 'QCD'.

	$\sqrt{s}$ (TeV)	Lower Limit ($\log s$) (mb)	QCD (Eikonal) (mb)	Upper Limit (Regge) (mb)
LHC	16	105 ± 1.2	107 ± 4	115
SSC	40	118 ± 1.2	121 ± 5	135

for the total cross sections at these accelerators. In order to get a measure of the accuracy of the predictions, they introduced the Regge Pole extrapolation as an *upper* bound (since it violates unitarity, and thus is too large), and the $\log s$ fit of Block and White[7] as a *lower* bound (since the 'QCD' prediction eventually goes as $\log^2 s$). Their collider predictions, tightly bounded, are shown in Table III. They predict $\sigma_{\rm tot}$ is 107 and 121 mb, at the LHC and SSC, respectively. Clearly, the future will be both productive and exciting.

References

1. UA4 Collaboration, D. Bernard *et al*, *Phys. Lett.* **B198**, 583 (1987).

2. M. M. Block and R. N. Cahn, *Rev. Mod. Phys.* **57**, 563 (1985).

3. H. A. Bethe, *Ann. Phys.* **3**, 190 (1958);
G. B. West and D. Yennie, Phys. Rev. **172**, 1413 (1968);
R. N. Cahn, *Z. Phys.* C **15**, 253 (1982).

4. E710 Collab., presented at the International Conference on Elastic and Diffractive Scattering (4th Blois Workshop), Elba, Italy, May 22, 1991.

5. CDF Collab., presented at the International Conference on Elastic and Diffractive Scattering (4th Blois Workshop), Elba, Italy, May 22, 1991.

6. A. Donnachie and P. V. Landshoff, *Nucl. Phys.* **B267**, 657(1986);
Nucl. Phys. **B348**, 297 (1991); Gordon Breach Science Publishers—*Particle World* **2**, 7 (1991);
P. Landshoff, *Nucl. Phys. (Proc. Suppl.)* **B12**, 397 (1990).

7. M. M. Block and A. R. White, presented at the International Conference on Elastic and Diffractive Scattering (4th Blois Workshop), Elba, Italy, May 22, 1991;
Northwestern University (N.U.H.E.P. Report No. 152, May, 1991);
Phys. Lett., in press (1991).

8. M. M. Block *et al*, *Phys Rev.* **D41**, 978 (1990).

9. M. M. Block, F. Halzen and B. Margolis, *Phys. Lett.* **B252**, 481 (1990).

10. K. Kang and A. R. White, *Phys. Rev.* **D42**, 835 (1990);
Phys. Lett. **B266**, 147 (1991).

11. P. D. B. Colllins, *"Regge Theory and High Energy Physics"* (Cambridge U. P., London, 1977); see also,
P. D. B. Colllins, F. D. Gault and A. Martin, *Nucl. Phys.* **B85**, 141 (1977).

12. E710 Collab., N. Amos *et al.* , *Phys. Lett.* **B247**, 127 (1990).

13. R. J. Eden, *Phys. Rev. Lett.* **16**, 39 (1966).

14. T. Kinoshita, in *"Perspectives in Modern Physics"*, edited by R. E. Marshak, (Wiley, New York), p. 211 (1966).

15. L. Lukaszuk and B. Nicolescu, *Lett. Nuovo Cimento* **8**, 405 (1973).

16. K. Kang and B. Nicolescu, *Phys. Rev.* **D11**, 2461 (1975).

17. D. Joynson *et al*, *Nuovo Cimento* **A30**, 345 (1975).

18. L. Durand and R. Lipes, *Phys. Rev. Lett.* **20**, 637 (1968).

19. T. T. Chou and C. N. Yang, *Phys. Rev.* **170**, 1591 (1968);
T. T. Chou and C. N. Yang, *Phys. Lett.* **B128**, 457 (1983).

20. M. Froissart, *Phys. Rev.* **123**, 1053 (1961).

21. H. Cheng and T. T. Wu, *Phys. Rev. Lett.* **24**, 1456 (1970).

22. M. Block, F. Halzen and B. Margolis, Northwestern University (N.U.H.E.P. Report No. 171, July, 1991);
Phys. Rev. **D**, in press (1991).

23. F. Auberson, T. Kinoshita and A. Martin, *Phys. Rev.* **D3**, 3185 (1971).

24. T. K. Gaisser, U. .P. Sukhatme and G. B. Yodh, *Phys. Rev.* **D36**, 1350 (1987).

END

DATE FILMED

01/27/92